

Genome Assembly of the Medicinal Plant *Voacanga thouarsii*

Clément Cuello ¹, Emily Amor Stander ¹, Hans J. Jansen², Thomas Dugé de Bernonville ^{1,1}, Arnaud Lanoue ¹, Nathalie Giglioli-Guivarc'h ¹, Nicolas Papon ³, Ron P. Dirks², Michael Krogh Jensen ⁴, Sarah Ellen O'Connor ⁵, Sébastien Besseau ¹, and Vincent Courdavault ^{1,*}

¹Biomolécules et Biotechnologies Végétales, EA2106, Université de Tours, 37200 Tours, France

²Future Genomics Technologies, 2333 BE Leiden, The Netherlands

³Univ Angers, Univ Brest, IRF, SFR ICAT, F-49000 Angers, France

⁴Novo Nordisk Foundation Center for Biosustainability, Technical University of Denmark, Kgs Lyngby, Denmark

⁵Department of Natural Product Biosynthesis, Max Planck Institute for Chemical Ecology, Jena 07745, Germany

¹Present address: Limagrain, Centre de Recherche, Route d'Ennezat, Chappes, France

*Corresponding author: E-mail: vincent.courdavault@univ-tours.fr.

Accepted: 22 October 2022

Abstract

The *Apocynaceae* tree *Voacanga thouarsii*, native to southern Africa and Madagascar, produces monoterpene indole alkaloids (MIA), which are specialized metabolites with a wide range of bioactive properties. *Voacanga* species mainly accumulate tabersonine in seeds making these species valuable medicinal plants currently used for industrial MIA production. Despite their importance, the MIA biosynthesis in *Voacanga* species remains poorly studied. Here, we report the first genome assembly and annotation of a *Voacanga* species. The combined assembly of Oxford Nanopore Technologies long-reads and Illumina short-reads resulted in 3,406 scaffolds with a total length of 1,354.26 Mb and an N50 of 3.04 Mb. A total of 33,300 protein-coding genes were predicted and functionally annotated. These genes were then used to establish gene families and to investigate gene family expansion and contraction across the phylogenetic tree. A transposable element (TE) analysis showed the highest proportion of TE in *Voacanga thouarsii* compared with all other MIA-producing plants. In a nutshell, this first reference genome of *V. thouarsii* will thus contribute to strengthen future comparative and evolutionary studies in MIA-producing plants leading to a better understanding of MIA pathway evolution. This will also allow the potential identification of new MIA biosynthetic genes for metabolic engineering purposes.

Significance

Voacanga species are major industrial resources of tabersonine, an important intermediate in the synthesis of aspidosperma-type monoterpene indole alkaloids (MIA), that are of high pharmaceutical importance. Despite their significant role in the pharmaceutical industry, no previous study reported genomic analysis of MIA metabolism in *Voacanga* species. Here, we provide the first annotated reference genome of a *Voacanga* species that, together with the previously published MIA-producing plant genomes, will help understand evolution and diversification of MIA in plants as well as identifying MIA biosynthetic genes to enrich the molecular MIA toolbox used for production of MIA in heterologous hosts.

© The Author(s) 2022. Published by Oxford University Press on behalf of Society for Molecular Biology and Evolution.

This is an Open Access article distributed under the terms of the Creative Commons Attribution-NonCommercial License (<https://creativecommons.org/licenses/by-nc/4.0/>), which permits non-commercial re-use, distribution, and reproduction in any medium, provided the original work is properly cited. For commercial re-use, please contact journals.permissions@oup.com

Key words: monoterpene indole alkaloids, tabersonine, wild frangipani.

Introduction

The wild frangipani, *Voacanga thouarsii*, is a small *Apocynaceae* tree native to southern Africa and Madagascar. *Apocynaceae* species are known to accumulate a broad spectrum of specialized metabolites including monoterpene indole alkaloids (MIA; Leeuwenberg, 1980). These compounds are part of the plant defense mechanisms to face both biotic and abiotic pressures (Dugé de Bernonville et al. 2015). Due to the high diversity of their bioactive properties, MIAs are active substances of many drugs such as antihypertensive and anticancer ones (O'Connor and Marseh, 2006; Macabeo et al. 2009).

MIAs originate from the condensation of secologanin and tryptamine yielding strictosidine followed by its subsequent decorations and/or cyclisation (De Luca et al. 1987; Maresh et al. 2007). Their biosynthetic pathways have extensively been studied over the last three decades mainly in *Catharanthus roseus* (as reviewed by Pan et al. 2016 and Kulagina et al. 2022). More than 100 MIAs have been reported in *Voacanga* species (see Hussain et al. 2012 for extensive review) including the valuable voacamine, resulting from the dimerization of vobasine and ibogaine (fig. 1A.iii). Voacamine is used in several African countries to fight malaria and also displays strong antimicrobial and cardiotoxic properties (Diavara et al. 1984; Ramanitrahambola et al. 2001). *Voacanga thouarsii* and *V. africana* also stands out for a high accumulation level of the aspidosperma-type MIA tabersonine (fig. 1A.ii) especially in seeds (Dzoyem et al. 2013; Kunesch et al. 1977; Rolland et al. 1975; Goldblatt et al. 1970). Tabersonine is a key intermediate in the synthesis of many important medicinal MIA (e.g., vindoline, pachysiphine). Even though these two *Voacanga* species are major industrial sources of tabersonine, the biosynthetic routes of their MIAs have not been studied to date. Here, we report the first *Voacanga* genome assembly. Together with the eight previously published MIA-producing plant genome (Stander et al. 2022), this new genome resource will increase our understanding of MIA diversification as well as the evolution of their biosynthetic pathways.

Results and Discussion

Genome Assembly and Annotation

Voacanga thouarsii was assembled into 3,451 contigs with an N50 of 2.91 Mb. The pilon-polished assembly consisted in 1,341.26-Mb distributed across 3,406 scaffolds with an

N50 of 3.04 Mb (table 1) and a GC content of 34.31%. Currently reported *Apocynaceae* assemblies (*Calotropis gigantea*, *Catharanthus roseus*, *Vinca minor*), ranging from 157.28 to 679.10 Mb, are smaller than the one reported here (table 1). The base-level QV of 36.8732, corresponding to more than 99.999% accuracy, and the k-mer completeness of 93.9624% are good indicators of the high quality of the assembled genome.

Based on the identification of core *Eudicotyledons* Benchmarking Universal Single-Copy Orthologs (BUSCO), the assembled genome is 97.1% complete (fig. 1B). Gene prediction with MAKER2 (Holt and Yandell, 2011) annotation tool identified 33,300 protein-coding genes in the assembled genome which is comparable to the previously published *Apocynaceae* species (table 1). Based on *Eudicotyledons* BUSCO, this predicted set of genes is 90.7% complete with a very low duplication rate (2.5%, fig. 1B).

The combination of BLASTP and BLASTX against UniProt database and hmmscan against the PFAM database led to the functional annotation of 65.7% of the predicted genes (21,890 of the 33,300 genes, fig. 1C, supplementary table S1, Supplementary Material online). To identify putative orthologs of MIA biosynthetic genes, we used functionally validated MIA pathway genes from *Catharanthus roseus*, *V. minor*, *Tabernanthe iboga*, *Gelsemium sempervirens* and *Rauwolfia* species to conduct BLAST searches considering hits of at least 90% coverage and 40% identity (supplementary tables S2-S3, Supplementary Material online). The most probable orthologues were then selected based on best hits and phylogeny analysis (supplementary table S4, Supplementary Material online). Based on this approach, we were able to identify putative orthologs with high confidences (76–94% protein identity) for almost 90% of terpenoids, iridoids, and MIA biosynthetic genes up to tabersonine. Interestingly, putative orthologs of genes from the terpenoids and early iridoid pathway tend to be more expressed in leaves while orthologs of genes from the late iridoid, indole, and central MIA pathways tend to be more expressed in roots, thus suggesting a specialization of MIA synthesis (supplementary table S4, Supplementary Material online). Very poor confidences were obtained for putative orthologs of the MIA pathway genes downstream of tabersonine (<64% protein identity). As an example, identity between orthologs is so weak that we were not able to discriminate putative orthologs of T16H and TEX. This thus suggests two possible evolution scenarios of the genes encoding tabersonine-modifying enzymes relying either on a wide diversification in plants accumulating several tabersonine-derived MIAs such as in

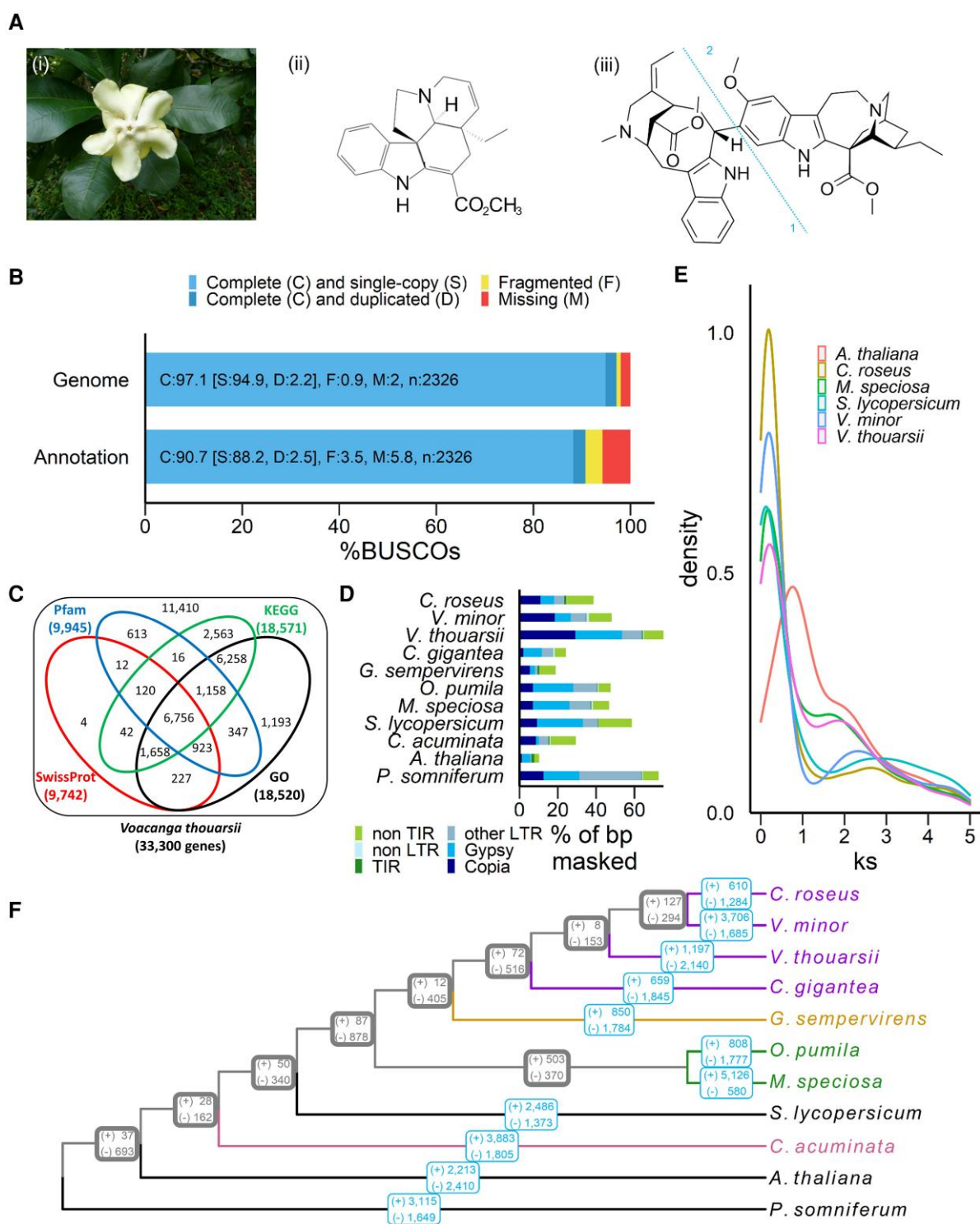


Fig. 1.—The annotated *Voacanga thouarsii* genome. (A) *Voacanga thouarsii* flowers (i) and the molecular structure of two main MIA: tabersonine (ii) and voacamine (iii) which results in the combination of a vobasine (1) and an ibogain (2). (B) BUSCO scores of genome and annotated genes. (C) Functional annotation of genes using SwissProt, Pfam, KEGG, and GO databases. (D) Transposable element proportion and classification. TIR: terminal inverted repeat, LTR: long terminal repeat, other LTR: LTR containing retrotransposons except for *Gypsy* and *Copia*, non-LTR: retrotransposons without LTR sequence, non TIR: DNA transposons without TIR sequence. (E) Synonymous substitution (Ks) rate distribution plot for *V. thouarsii* orthologs compared with other eudicots. (F) Phylogenetic tree of *V. thouarsii* and 10 other species including three *Apocynaceae* (purple: *C. roseus*, *V. minor*, *C. gigantea*), one *Gelsemiaceae* (yellow: *G. sempervirens*), two *Rubiaceae* (green: *O. pumila*, *M. speciosa*) and one *Cornales* (pink: *C. acuminata*). Gene family expansion (+) and contraction (–) were calculated using Cafe5 in each lineage (light bordered blue boxes) and in internal nodes of ancestral population for each taxon (thick bordered grey boxes).

Table 1

Genome assembly metrics

Species	Family	Assembly size (Mb)	No. of scaff. ^a	N50 (Mb)	Protein -coding genes	BUSCO C [S; D]; F; M ^b	Ref.
<i>A. thaliana</i>	Bras.	119.67	7	23.46	27,564	99.6 [98.8; 0.8]; 0.1; 0.3	[1]
<i>C. gigantea</i>	Apo.	157.28	1,536	0.81	18,197	93.0 [91.6; 1.4]; 1.7; 5.3	[2]
<i>C. acuminata</i>	Corn.	414.95	775	18.28	27,940	98.2 [90.5; 2.2]; 0.5; 1.3	[3]
<i>C. roseus</i>	Apo.	541.13	2,090	2.58	34,363	97.0 [95.5; 1.5]; 1.3; 1.7	[4]
<i>G. sempervirens</i>	Gel.	244.39	3,352	0.41	22,617	96.5 [95.1; 1.4]; 0.9; 2.6	[4]
<i>M. speciosa</i>	Rub.	1,122.52	40,370	1.02	55,746	91.2 [37.7; 53.5]; 5.0; 3.8	[5]
<i>O. pumila</i>	Rub.	440.32	13	40.57	91,162	96.9 [93.7; 3.2]; 0.9; 2.2	[6]
<i>P. somniferum</i>	Pap.	2,715.53	34,381	204.47	62,934	94.8 [9.2; 85.6]; 1.2; 4.0	[7]
<i>S. lycopersicum</i>	Solan.	782.52	13	65.27	34,075	98.5 [97.6; 0.9]; 0.6; 0.9	[8]
<i>V. minor</i>	Apo.	679.10	296	5.97	29,624	96.9 [60.3; 36.6]; 1.1; 2.0	[9]
<i>V. thourasii</i>	Apo.	1,351.26	3,406	3.04	33,300	97.1 [94.9; 2.2]; 0.9; 2.0	This study

^anumber of scaffolds; ^bBUSCO scores (genome mode) % Complete [% Complete and single-copy; % Complete and Duplicated]; % Fragmented; % Missing ($n = 2,326$).

A. thaliana: *Arabidopsis thaliana*, *C. gigantea*: *Calotropis gigantea*, *C. acuminata*: *Camptotheca acuminata*, *C. roseus*: *Catharanthus roseus*, *G. sempervirens*: *Gelsemium sempervirens*, *M. speciosa*: *Myrtagyna speciosa*, *O. pumila*: *Ophiorrhiza pumila*, *P. somniferum*: *Papaver somniferum*, *S. lycopersicum*: *Solanum lycopersicum*, *V. minor*: *Vinca minor*, *V. thourasii*: *Voacanga thourasii*.

Bras.: Brassicaceae, Apo.: Apocynaceae, Corn.: Cornales, Gel.: Gelsemiaceae, Rub.: Rubiaceae Pap.: Papaveraceae, Solan.: Solanaceae.

[1] Lamesh et al. 2012; [2] Hoopes et al. 2018; [3] Kang et al. 2021; [4] Franke et al. 2019; [5] Brose et al. 2021; [6] Rai et al. 2021; [7] Guo et al. 2018; [8] Hosmani et al. 2019; [9] Stander et al. 2022.

Catharanthus roseus or to their non-functionalization in *V. thourasii* leading to their loss and the high accumulation of tabersonine. Indeed, such an evolutionary process has already been described in benzoxazinoid biosynthesis (Frey et al. 2009). By contrast, confident gene orthologs of the voacamine biosynthesis branch were found in agreement with its accumulation in *Voacanga* species (Hussain et al. 2012).

Transposable Element Annotation

Transposable elements (TE) have well-known roles in genome evolution, genetic instability and gene expression regulation (Sahebi et al. 2018), prompting us to analyze TE composition in *V. thourasii*. This analysis showed that 75.16% of the genome consists of TE (fig. 1D), which mainly corresponds to long terminal repeat retrotransposons (63.9% of total TE) with a similar proportion of *Copia* and *Gypsy* elements (29.1% and 24.4%, respectively, fig. 1D). Interestingly, *V. thourasii* genome displayed the highest proportion of TE compared with all other MIA-producing plants studied that could be a reason for the low scaffolding levels. Indeed, *V. thourasii* genome is composed of 3,406 scaffolds when all other *Apocynaceae* genomes we studied ranged between 296 and 2,090 scaffolds (table 1). Moreover, a similar phenomenon is observed with *Papaver somniferum* genome, which has a similar TE content to *V. thourasii* (72.58%), a genome size that is almost twice as large and a high number of scaffolds (table 1, fig. 1D).

Whole-Genome Duplication Analysis

We then searched for whole-genome duplication (WGD) events by calculating synonymous substitution per synonymous sites (Ks) for paralogous gene pairs across

different plant species (fig. 1E). Here, we detected the conserved γ whole-genome triplication (Jiao et al. 2012) common to all eudicots at a Ks of around 2 in all studied species. No other secondary peak could be observed indicating that *V. thourasii* did not go through any additional WGD.

Comparison of Orthologous Genes

A maximum-likelihood phylogenetic tree of the 11 studied species was constructed from 680 single-copy orthogroups obtained from OrthoFinder. Lineage-specific (fig. 1F, blue) and ancestral (fig. 1F, grey) gene family evolution was determined using Cafe5. Even though a similar number of genes was annotated in *V. Thourasii* genome compared with other *Apocynaceae*, *V. thourasii* showed the highest decrease in orthogroups (2,140) among all investigated MIA-producing plants. Such a difference may result from putative variations in the copy-number of several genes. For instance, 404 *V. thourasii* genes were annotated as putative cytochrome P450 while 225 cytochrome P450 are annotated in *Catharanthus roseus* genome (Franke et al. 2019). Among the 2,140 decreased orthogroups, 1,608 orthogroups completely disappeared in *V. thourasii* including 952 existing in the three studied *Apocynaceae* (supplementary table S5, Supplementary Material online). These losses could be linked to the high proportion of TE in *V. thourasii* compared with other *Apocynaceae*, in agreement with their key roles in genome evolution (Catlin and Josephs, 2022). Indeed, several studies conducted in plants (Tang et al. 2012; Bariah et al. 2020; Boatwright et al. 2021) and animals (Pantartz et al. 2018; Bourgeois et al. 2020) have highlighted the impact of TE on the loss of functional genes. Such dynamics could also explain the differences in

MIAs from *Voacanga* species compared with other MIA-producing plants.

Conclusions

Here, we described the genome of the wild frangipani, *Voacanga thouarsii*, which will be a valuable resource for future evolutionary and functional studies. Our genomic analysis showed that despite some similarities (e.g., similar gene content, absence of post- γ whole-genome duplication), *V. thouarsii* genome displays specific genomic features such as a higher TE content and a bigger size compared with other *Apocynaceae*. This new *Apocynaceae* genome thereby paves the way for a better understanding of MIA biosynthesis as well as the identification of new and/or more efficient MIA biosynthetic enzymes that can be used in the developing yeast cell factories producing MIAs (Guirimand et al. 2021; Kulagina et al. 2021; Zhang et al. 2022).

Materials and Methods

Sample Collection, DNA Extraction and Sequencing

Voacanga thouarsii seeds were obtained from Boutique Végétale (<https://boutique-vegetale.com/>). Seeds were soaked for 16 h before sowing. Plant were greenhouse-grown for three months before sampling. DNA was extracted from *V. thouarsii* leaves using Qiagen Plant DNeasy kit (Qiagen, Hilden, Germany) following the manufacturer's instructions. Illumina sequencing library were built using the Nextera Flex kit (Illumina, San Diego, USA) by Future Genomics Technologies (Leiden, The Netherlands) and subsequently sequenced in paired-end mode (2 × 150 bp) using Illumina NovaSeq 6,000 technology. Future Genomics Technologies (Leiden, The Netherlands) constructed ONT library using ONT 1D ligation sequencing kit (Oxford Nanopore Technologies Ltd, Oxford, United-Kingdom) subsequently sequenced on Nanopore PromethION flowcell (Oxford Nanopore Technologies Ltd, Oxford, United-Kingdom) with the guppy version 4.0.11 high-accuracy basecaller. A total of 281,539,400 reads were obtained from the Illumina NovaSeq 6,000 sequencing and 11,390,893 from the ONT PromethION sequencing.

RNA Sequencing and Assembly

RNA was extracted from liquid nitrogen flash-frozen roots, young and old leaves using NucleoSpin RNA Plant and Fungi mini kit (Macherey-Nagel, Düren, Germany) and purified using RNase-free TURBO DNase set (Thermo Fisher Scientific, Illkirch-Graffenstaden, France), both according to the suppliers' instructions. RNA library construction and sequencing was performed at FGtech using Illumina

NovaSeq 6,000 technology. Raw RNA-seq data have been deposited under the SRA accession numbers SRR19972991, SRR19972992, and SRR19972993. Transcriptome was assembled using CLC assembler (v.4.4.1) with a word size of 60 and a bubble size of 250.

De Novo Genome Assembly, Gene Model Prediction and Gene Functional Annotation

The *V. thouarsii* genome assembly and gene model prediction were performed by Future Genomics Technologies (Leiden, The Netherlands). Adapters were removed using porechop (Wick et al. 2017). ONT reads were first assembled into contig using Flye assembler (v.2.8.2, Kolmogorov et al. 2019) with the following options: `-min-overlap 10,000 -i 2`. Redundant contigs were removed using purge_haplotigs (v.1.1.0) followed by two rounds of polishing with Illumina paired-end reads using pilon (v.1.23, Walker et al. 2014). Gene modeling was performed using MAKER2 pipeline (v.3.01.02, Holt and Yandell, 2011) using CLC assembled transcriptome as evidence. Putative function for each gene model was then assigned via a combination of similarity search (BLASTX of predicted transcript and BLASTP of TransDecoder (v.5.5.0, Haas et al. 2013) predicted ORFs against the UniProt database) and hmmscan (v.3.1b2, Finn et al. 2011) against the PFAM database (<https://pfam.xfam.org/>).

Assembly Completeness Assessment

Assembly quality was assessed using the stat program from BBMap tool (v.38.94, Bushnell, 2014). Complementary quality metrics were obtained from merqury (v. 1.3, Rhie et al. 2020). Briefly, 20-mers database was constructed from Illumina short-reads using count function from meryl (v.1.3, Koren et al. 2017). K-mer survival rate was then used to estimate base-level consensus quality score (QV). K-mer completeness was evaluated considering the fraction of reliable k-mers in read database also found in the assembly. Genome and gene models completeness were assessed by applying Benchmarking Universal Single-Copy Orthologs (BUSCO v.5.2.2, Simão et al. 2015) with default settings using a plant-specific database of 2,326 single-copy orthologs (eudicots_odb10). Gene models statistics were obtained using agat_sp_statistics from the AGAT package (v.0.8.0, Dainat, 2022).

Transposable Elements Prediction and Annotation

Extensive de novo TE annotator (EDTA v.1.9.5, Ou et al. 2019) was used to identify and annotate transposable element (TE). Sensitive option using RepeatModeler (v.2.0.1, Smit and Hubley, 2015) was used to identify remaining TEs. Classification consistency was evaluated using evaluate option. alluniRefprexp082813 curated database was used to perform TE annotation.

Whole-Genome Duplication Analysis

To infer whole-genome duplication (WGD) events, transcript sequences of *V. thouarsii*, *V. minor* (Stander et al. 2022), *Arabidopsis thaliana* (Lamesh et al. 2012), *Catharanthus roseus* (Franke et al. 2019), *Mytragyna speciosa* (Brose et al. 2021), *Solanum lycopersicum* (Hosmani et al. 2019), *Camptotheca acuminata* (Kang et al. 2021), *Calotropis gigantea* (Hoopes et al. 2018), *G. sempervirens* (Franke et al. 2019), *Ophiorrhiza pumila* (Rai et al. 2021), and *P. somniferum* (Guo et al. 2018) were input to the DupPipe pipeline (Barker et al. 2010). For each dataset, discontinuous MegaBLAST (Ma et al. 2002, Zhang et al. 2004) was used to identify duplicated gene pairs (40% sequence similarity over 300 bp). For each gene pair, the open reading frame was inferred from the NCBI's plant RefSeq protein database (May 21, 2021) using BLASTx (v.2.6.0-1, Camacho et al. 2009). Only the best hit sequence was retained (sequence similarity threshold: 30% over 150 aa). DNA sequence alignment against its best hit homologous protein sequence and its translation was performed using GeneWise (Birney et al. 2004). Resulting amino acid sequences for each gene pair were aligned using MUSCLE (v.3.6, Edgar, 2004). This alignment further guided nucleic acid alignment using RevTrans (v.1.4, Wernersson and Pedersen, 2003). Codeml's F3 × 4 model from PAML package (v.4.9, Yang, 1997) was used to calculate substitutions per synonymous site (Ks) and thus determine divergence times between gene pairs.

Phylogenetic Tree Reconstruction

Gene families were constructed by comparing the protein sequences of *V. thouarsii* with ten other plant species: *V. minor* (Stander et al. 2022), *A. thaliana* (Lamesh et al. 2012), *Catharanthus roseus* (Franke et al. 2019), *M. speciosa* (Brose et al. 2021), *S. lycopersicum* (Hosmani et al. 2019), *C. acuminata* (Kang et al. 2021), *Calotropis gigantea* (Hoopes et al. 2018), *G. sempervirens* (Franke et al. 2019), *O. pumila* (Rai et al. 2021) and *P. somniferum* (Guo et al. 2018). Protein sequences of less than 30 amino acids were removed. For each species, the longest representative protein was selected in each CD-HIT (v.4.7; Fu et al. 2012) cluster. These sequences were then used as input for OrthoFinder (v.2.5.4; Emms and Kelly, 2019) using the following parameters: -S diamond -M msa -A muscle -T raxml-ng. 680 single-copy orthogroups were used to build a maximum-likelihood phylogenetic tree. Orthogroup gain and expansion were determined across the phylogenetic tree using Cafe5 (v.4.2.1, Mendes et al. 2021).

Transcript Abundance Estimation

Reads were pseudo-aligned onto the predicted transcripts and counted using Salmon (v.0.6.0; Patro et al. 2017) using

-biasCorrect and -vbo options. Abundance estimates were established as transcripts per million (TPM) and are presented in [supplementary table S6, Supplementary Material](#) online.

Supplementary Material

Supplementary data are available online at *Genome Biology and Evolution* online.

Acknowledgements

We thank access and support to the CCSC computing resources (Cascimodot Federation, CNRS, Orléans). We acknowledge funding from the EU Horizon 2020 research and innovation program (MIAMi project-Grant agreement N°814645), ARD-CVL Biopharmaceutical program of the Région Centre Val de Loire (ETOPOCentre project), and ANR (project MIACYC—ANR-20-CE43-0010).

The authors benefitted from the use of the cluster at the Centre de Calcul Scientifique en région Centre-Val de Loire.

Author Contributions

S.E.O., M.K.J., T.D.D.B., S.B., V.C. designed the research. E.A.S., R.P.D. and H.J.J. acquired the data. C.C., E.A.S., H.J.J., A.L., N.G.G., N.P. and R.P.D. analyzed the data. C.C., S.B. and V.C. wrote the article. All authors read and approved the final manuscript.

Data Availability

The annotated genome has been deposited in the NCBI database under the Bioproject accession number PRJNA860765. RNAseq raw reads have been deposited in the NCBI database under the SRA accession numbers SRR19972991, SRR19972992, and SRR19972993. Genome annotation predicted transcripts and proteins, and transcript expression abundances are available on figshare: <https://doi.org/10.6084/m9.figshare.20223093.v1>

Funding Information

This work was supported by Horizon 2020 research and innovation program [MIAMi project-Grant agreement N 814645]; ARD CVL Biopharmaceutical program of the Région Centre-Val de Loire [ETOPOCentre project]; and ANR (project MIACYC—ANR-20-CE43-0010).

Conflict of Interest

Ron Dirks and Hans Jensen are CEO and CTO of Future Genomics Technologies, respectively.

Literature Cited

- Bariah I, Keidar-Friedman D, Kashkush K. 2020. Where the wild things are: transposable elements as drivers of structural and functional variations in the wheat genome. *Front Plant Sci.* 11:585515.
- Barker MS, et al. 2010. Evopipes.net: bioinformatic tools for ecological and evolutionary genomics. *Evol Bioinforma Online* 6:143–149.
- Birney E, Clamp M, Durbin R. 2004. Genewise and genomewise. *Genome Res.* 14:988–995.
- Boatwright JL, et al. 2021. Trajectories of homoeolog-specific expression in allotetraploid *Tragopogon castellanus* populations of independent origins. *Front Plant Sci.* 12:679047.
- Bourgeois Y, Ruggiero RP, Hariyani I, Boissinot S. 2020. Disentangling the determinants of transposable elements dynamics in vertebrate genomes using empirical evidences and simulations. *PLoS Genet.* 16:e1009082.
- Brose J, et al. 2021. The *Mitragyna speciosa* (kratom) genome: a resource for data-mining potent pharmaceuticals that impact human health. *G3 (Bethesda)* 11:jkab058.
- Bushnell B (2014). BBMap: a fast, accurate, splice-aware aligner. (No. LBNL-7065E). Berkeley (CA): Lawrence Berkeley National Lab. (LBNL).
- Camacho C, et al. 2009. BLAST+: architecture and applications. *BMC Bioinf.* 10:421.
- Caputi L, et al. 2018. Missing enzymes in the biosynthesis of the anticancer drug vinblastine in Madagascar periwinkle. *Science* 360:1235–1239.
- Catlin NS, Josephs EB. 2022. The important contribution of transposable elements to phenotypic variation and evolution. *Curr Opin Plant Biol.* 65:102140.
- Dainat J, Hereñú D, LucileSol, pascal-git.2022. NBISweden/AGAT: AGAT-v0.8.1. Zenodo. <https://zenodo.org/record/5834795#.Y2jXNNLMKV4>.
- De Luca V, Balsevich J, Tyler RT, Kurz WGW. 1987. Characterization of a novel N-methyltransferase (NMT) from *Catharanthus roseus* plants. *Plant Cell Rep.* 6:458–461.
- Diavara D, Pyuskyulev B, Kuzmanov B. 1984. Alkaloid-bearing plants in the flora of Guinea. Alkaloids from *Voacanga africana* stapf. *Izvestiya po Khimiya* 17:364–371.
- Dugé de Bernonville T, et al. 2015. Phytochemical genomics of the Madagascar periwinkle: unravelling the last twists of the alkaloid engine. *Phytochemistry* 113:9–23.
- Dzoyem JP, Tshikalange E, Kuete V. 2013. Medicinal plants market and industry in Africa. In: Kuete V, editors. *Medicinal plant research in Africa—pharmacology and chemistry*: Elsevier. p. 859–890.
- Edgar RC. 2004. MUSCLE: a multiple sequence alignment method with reduced time and space complexity. *BMC Bioinf.* 5:113.
- Emms DM, Kelly S. 2019. Orthofinder: phylogenetic orthology inference for comparative genomics. *Genome Biol.* 20.
- Finn RD, Clements J, Eddy SR. 2011. HMMER Web server: interactive sequence similarity searching. *Nucleic Acids Res.* 39:W29–W37.
- Franke J, et al. 2019. Gene discovery in *Gelsemium* highlights conserved gene clusters in monoterpene indole alkaloid biosynthesis. *ChemBioChem.* 20:83–87.
- Frey M, Schullehner K, Dick R, Fiesselmann A, Gierl A. 2009. Benzoxazinoid biosynthesis, a model for evolution of secondary metabolic pathways in plants. *Phytochemistry* 70:1645–1651.
- Fu L, Niu B, Zhu Z, Wu S, Li W. 2012. CD-HIT: accelerated for clustering the next-generation sequencing data. *Bioinformatics* 28:3150–3152.
- Goldblatt A, Hootele C, Pecher J. 1970. Indole alkaloids. XXIII. Alkaloids of *Voacanga thouarsii*. *Phytochemistry* 9:1293–1298.
- Guirimand G, Julagina N, Papon N, Hasunuma T, Courdavault V. 2021. T innovative tools and strategies for optimizing yeast cell factories. *Trends Biotechnol* 39:488–504.
- Guo L, et al. 2018. The opium poppy genome and morphinan production. *Science* 362:343–347.
- Haas BJ, et al. 2013. De novo transcript sequence reconstruction from RNA-seq: reference generation and analysis with TRinity. *Nat Protoc.* 8.
- Holt C, Yandell M. 2011. MAKER2: an annotation pipeline and genome-database management tool for second-generation genome projects. *BMC Bioinf.* 12:491.
- Hoopes GM, et al. 2018. Genome assembly and annotation of the medicinal plant *Calotropis gigantea*, a producer of anticancer and antimalarial cardenolides. *G3 (Bethesda)* 8:385–391.
- Hosmani PS, et al. 2019. An improved de novo assembly and annotation of the tomato reference genome using single-molecule sequencing, hi-C proximity ligation and optical maps.
- Hussain H, Hussain J, Al-Harrasi A, Green IR. 2012. Chemistry and biology of the genus *Voacanga*. *Pharm Biol.* 50:1183–1193.
- Jiao Y, et al. 2012. A genome triplication associated with early diversification of the core eudicots. *Genome Biol.* 13:R3–R3.
- Kang M, et al. 2021. A chromosome-level *Camptotheca acuminata* genome assembly provides insights into the evolutionary origin of camptothecin biosynthesis. *Nat Commun.* 12:1–12.
- Kolmogorov M, Yuan J, Lin Y, Pevzner PA. 2019. Assembly of long, error-prone reads using repeat graphs. *Nat Biotechnol.* 37:540–546.
- Koren S, et al. 2018. De novo assembly of haplotype-resolved genomes with trio binning. *Nat Biotechnol.* 36(12):1174–1182. doi: 10.1038/nbt.4277.
- Kulagina N, et al. 2021. Enhanced bioproduction of anticancer precursor vindoline by yeast cell factories. *Microb Biotechnol* 14:2693–2699.
- Kulagina N, Méteignier LV, Papon N, O'Connor SE, Courdavault V. 2022. More than a Catharanthus plant: a multicellular and pluri-organelle alkaloid-producing factory. *Curr Opin Plant Biol.* 67:102200.
- Kunesch N, et al. 1977. Alkaloids of *Voacanga*. XVIII. Alkaloids of *Callichilia subsessilis*. IV. Organic natural products. 165. The structure of bisindoline alkaloids of a novel type. *Helv Chim Acta* 60:2854–2859.
- Lamesch P, et al. 2012. The Arabidopsis information resource (TAIR): improved gene annotation and new tools. *Nucleic Acids Res.* 40:D1202–D1210.
- Leeuwenberg AJM. 1980. The taxonomic position of some genera in the *Loganiaceae*, *Apocynaceae*, and *Rubiaceae*, related families which contain indole alkaloids. In: Phillipson JD and Zenk MH, editors. *Indole and biogenetically related alkaloids*: Academic Press. p. 1–10.
- Ma B, Tromp J, Li M. 2002. Patternhunter: faster and more sensitive homology search. *Bioinformatics* 18:440–445.
- Macabeo AP, Alejandro GJ, Hallare AV, Vidar WS, Villaflores OB. 2009. Phytochemical survey and pharmacological activities of the indole alkaloids in the genus *Voacanga* thouars (Apocynaceae)—an update. *Pharmacogn Rev.* 3:132–142.
- Maresh JJ, et al. 2007. Strictosidine synthase: mechanism of a pictet-spengler catalyzing enzyme. *J Am Chem Soc.* 130:710–723.
- Mendes FK, Vanderpool D, Fulton B, Hahn MW. 2021. CAFE 5 Models variation in evolutionary rates among gene families. *Bioinformatics* 36:5516–5518.
- Mistry V, Darji S, Tiwari P, Sharma A. 2022. Engineering *Catharanthus roseus* monoterpene indole alkaloid pathway in yeast. *Appl Microbiol Biotechnol* 106:2337–2347.
- O'Connor SE, Maresh JJ. 2006. Chemistry and biology of monoterpene indole alkaloid biosynthesis. *Nat Prod Rep.* 23:532–547.
- Ou S, et al. 2019. Benchmarking transposable element annotation methods for creation of a streamlined, comprehensive pipeline. *Genome Biol.* 20:275.

- Pan Q, Mustafa NR, Tang K, Choi YH, Verpoorte R. 2016. Monoterpenoid indole alkaloids biosynthesis and its regulation in *Catharanthus roseus*: a literature review from genes to metabolites. *Phytochem Rev* 15:221–250.
- Pantzartzis C, Pergner J, Kozmik Z. 2018. The role of transposable elements in functional evolution of amphioxus genome: the case of opsin gene family. *Sci Rep*. 8:2506.
- Patro R, Duggal G, Love MI, Irizarry RA, Kingsford C. 2017. Salmon provides fast and bias-aware quantification of transcript expression. *Nat Methods* 14:417–419.
- Rai A, et al. 2021. Chromosome-level genome assembly of *Ophiorrhiza pumila* reveals the evolution of camptothecin biosynthesis. *Nat Commun*. 12:1–19.
- Ramanitrahasimbola D, et al. 2001. Biological activities of the plant-derived bisindole voacamine with reference to malaria. *Phytother Res*. 15:30–33.
- Rhie A, Walenz BP, Koren S, Phillippy AM. 2020. Merqury: reference-free quality, completeness, and phasing assessment for genome assemblies. *Genome Biol*. 21:245. doi:10.1186/s13059-020-02134-9.
- Rolland Y, Kunesch N, Libot F, Poisson J, Budzikiewicz H. 1975. Alkaloids of Voacanga. XV. Structure of new alkaloids from the leaves of *Voacanga thouarsii*. *Bull Soc Chim Fr*. 11:2503–2506.
- Sahebi M, et al. 2018. Contribution of transposable elements in the plant's Genome. *Gene* 665:155–166.
- Simão FA, Waterhouse RM, Ioannidis P, Kriventseva EV, Zdobnov EM. 2015. BUSCO: assessing genome assembly and annotation completeness with single-copy orthologs. *Bioinformatics* 31:3210–3212.
- Smit AFA, Hubley R. 2015. RepeatModeler Open-1.0. <http://www.repeatmasker.org>.
- Stander EA, et al. 2022. The *Vinca minor* genome highlights conserved evolutionary traits in monoterpene indole alkaloid synthesis. G3 (Bethesda):jkac268.
- Tang H, et al. 2012. Altered patterns of fractionation and exon deletions in *Brassica rapa* support a two-step model of paleohexaploidy. *Genetics* 190:1563–1574.
- Walker BJ, et al. 2014. Pilon: an integrated tool for comprehensive microbial variant detection and genome assembly improvement. *PLoS One* 9:e112963–944.
- Wernersson R, Pedersen AG. 2003. Revtrans: multiple alignment of coding DNA from aligned amino acid sequences. *Nucleic Acids Res*. 31:3537–3539.
- Wick RR, Judd LM, Gorrie CL, Holt KE. 2017. Completing bacterial genome assemblies with multiplex MinION sequencing. *Microb Genom* 3:e000132.
- Yang Z. 1997. PAML: a program package for phylogenetic analysis by maximum likelihood. *Bioinformatics* 13:555–556.
- Zhang J, et al. 2022. A microbial supply chain for production of the anti-cancer drug vinblastine. *Nature* 609:341–347.
- Zhang Z, Schwartz S, Wagner L, Miller W. 2004. A greedy algorithm for aligning DNA sequences. *J Comput Biol*. 7:203–214.

Associate editor: Maud Tenaillon